

Fuzzy Logic Control Based Maximum Power Point Tracking for Three-Port Bidirectional DC-DC Converter with Photovoltaic-Battery System

^[1] A Devakumar, ^[2] R Narendra Rao
^[1] PG Scholar, ^[2] Lecturer
^[2] Dept. of EEE, JNTUCEP, Pulivendula.

Abstract— In this paper fuzzy logic controller (FLC) based maximum power point tracking (MPPT) for a three-port bidirectional isolated dc-dc converter proposed for power management to photovoltaic-Battery sources. This converter has a benefit of using smallest amount of switches which reduces the switching losses. The inductor-capacitor-inductor (LCL) resonant circuit realized to achieve soft switching. The converter is modelled to instantaneous power management of photovoltaic (PV) panel, battery and load. The proposed MPPT based on FLC is capable of attaining maximum power from PV panel when solar radiation available. The charging and discharging controller of the battery works when the extra energy and power deficiency with respect to the load, respectively. The presentation of fuzzy logic with numerous membership function (MF) is analyzed to develop the MPPT. Simulation results shows that performance of FLC based MPPT is better than conservative perturb and observe (P&O) MPPT.

Index Terms— Battery, fuzzy logic, isolated dc-dc converter, photovoltaic (PV), soft switching.

INTRODUCTION:

In present days to add multiple dc energy sources of diverse types to a power grid, many autonomous dc-dc converters are generally used to step up the time changing low-level source voltages to a continual high-level voltage. For this purpose preferred solution is multi-port dc-dc converters, due to the advantages of using smaller amount components, low cost, higher power density, and higher efficiency [1].

The multi-port converter configuration can be categorized into two categories: nonisolated topologies and isolated topologies [2]. In the applications when it requires lower voltage regulation ratio, Nonisolated converters are generally used, which does not have a transformer. Isolated converters are used in applications where it requires a higher voltage regulation percentage is required, which contain a transformer, are preferred [3].

Present used different types of isolated multi-port topologies are full-bridge, half-bridge and single switch converter. In isolated full-bridge converter [3], which uses four power switches which are controllable for every single source; the isolated half-bridge converter [4], which practices two switches for every single source; and the isolated single-switch converter [5], in which it only uses single switch for every single source. To manage the interruption of photovoltaic and wind type dc energy sources, it is required to use energy storage, such as battery. For this, it is required

that minimum a single port of the multi-port converter is bidirectional. Before cited topologies are unidirectional and cannot meet requirement of such applications.

In some of the bidirectional topologies, such as full-bridge, and half-bridge, topologies, have been proposed. As above mentioned two topologies utilizes more switches with complex drive and control circuits. In recent times, a new three-port topology has been used, by addition of one middle branch to the conventional half-bridge converter [6]. It uses less number of switches than the half-bridge topology and can attain the soft switching for all main switches. However, the primary source side voltage should be maintained high to charging and discharging of the battery within a given switching period. Such type of high switching frequency shows a pessimistic effect on lifetime of the battery.

This paper has a novel isolated three-port dc-dc converter. It contains an inductor-capacitor-inductor (LCL)-resonant circuit to achieve zero-current switching (ZCS) for main switch. Compared with the converter in [7] it uses five controllable switches, this converter only use three switches. In this work, the converter is applied for real-time power managing of a photo-voltaic (PV) system with a battery.

In this paper new MPPT based on fuzzy logic control [8] is proposed for the PV panel to produce the maximum power from the given dc-dc converter. A charging-discharging controller is applied to control the battery to either absorb the excess power generated by the PV panel or supply the

undersupplied power required by the load. The results of proposed MPPT based on FLC is compared with the P&O MPPT. Simulation are carried in the MATLAB/Simulink.

II. TOPOLOGY AND WORKING PRINCIPLE OF THE CONVERTER

A. Topology of Converter

The three-port dc-dc converter circuit diagram is shown in Fig. 1, which is having of a low voltage(LV) side circuit and a high voltage(HV) side circuit connected by a high-frequency

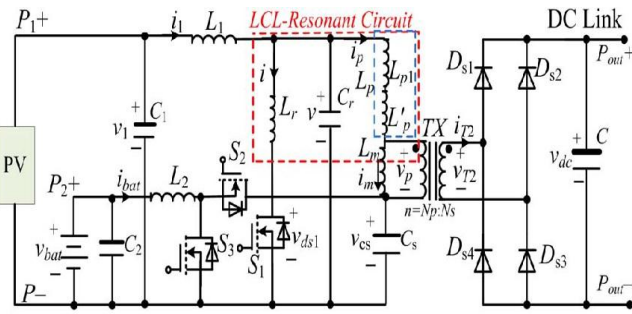


Fig. 1. Three-port bidirectional isolated dc-dc converter

transformer. The LV side having of two ports, an energy storing capacitor C_s . The LV side having a primary winding of the transformer, and an LCL-resonant circuit which consisting of two inductors L_r , L_p and a capacitor C_r , where L_p comprises the additional inductance L_{p1} and the leakage inductance of the transformer L'_p . The HV side consists of the secondary winding of the transformer and a full-bridge rectifier circuit employed with the diodes $D_{s1} \sim D_{s4}$. Turns ratio of the transformer is well-defined as: $n = N_p/N_s$, where N_p and N_s denote the numbers of turns of the primary side and secondary side windings, respectively. Among the switches, S_1 is the leading switch because it not only controls the power produced by the source connected to Port 1 (P_1) but also changes the current direction flowing during the transformer.

The two ports on the LV side are connected to the PV panel and a battery. For analysis, the given converter is analyzed by using two distinct converters: one is a single-switch LCL resonant converter [9], and the other is the battery-related buck-boost converter, which consisting of L_2 , S_2 , and S_3 .

B. Single-Switch LCL-Resonant Converter for PV Panel

In switching times, the voltages over C_1 and C_s can be taken as consistent values. Mostly, in the steady state, $V_{C_s} = V_1$, where V_1 is the output voltage of the PV panel. The converter has diverse operating modes relies upon the conditions of the switch S_1 and the resonant circuit. The differential equations for the resonant circuit in Mode k ($k = 1, \dots$) are

$$v = L_r^{(k)} \cdot \frac{di_r^{(k)}}{dt} \tag{1}$$

$$i_1 = C_r \cdot \frac{dv}{dt} + i_r^{(k)} \tag{2}$$

Where

- v = the voltage across capacitor C_r ;
- $L_r^{(k)}$ = the equivalent resonant inductance in k^{th} mode
- $i_r^{(k)}$ = the current through the equivalent resonant inductor in k^{th} mode.

Then, v can be derived from (1), (2) and has the following form:

$$v(t) = A^{(k)} \cos[\omega^{(k)}(t-t_k)] + B^{(k)} \sin[\omega^{(k)}(t-t_k)] + V^{(k)} \tag{3}$$

Where

$$\omega^{(k)} = \frac{1}{\sqrt{L_r^{(k)} \cdot C_r}} \tag{4}$$

is the resonant frequency in Mode k ; $V^{(k)}$ is the particular solution of (1) in Mode k , and $A^{(k)}$ and $B^{(k)}$ are coefficients, which can be articulated as follows:

$$A^{(k)} = v(t_k) - V^{(k)} \tag{5}$$

$$B^{(k)} = \frac{I_1 - i_p(t_k) - i(t_k)}{\omega^{(k)} \cdot C_r} \tag{6}$$

Where

$v(t_k)$ = voltage across the capacitor C_r at time t_k .

I_1 = current through inductor L_1 at time t_k .

$i_p(t_k)$ = current through inductor L_p at time t_k .

$i(t_k)$ = current through inductor L_r at time t_k .

When switch S_1 is on, L_r and L_p resonate with C_r , the current through inductor L_r rises, and the voltage of the capacitor C_r declines. Due to the presence of L_r , the current through the switch S_1 increases gradually, so that the switch is turned on under a low di/dt condition.

There are five inductances L_1, L_2, L_r, L_{p1} , and L_m in the converter that must to be properly calculated. L_m is calculated based on the following critical inductance L_{mc} :

$$L_{mc} = \frac{V_T \cdot T}{4 \cdot I_{m,pk}} \quad (7)$$

Where

T = the switching period of the switch S_1 ;

$I_{m,pk}$ = the peak current through the magnetizing inductor.

In this paper, the root-mean-square (RMS) value of the magnetization current is considered as 2% of the RMS value of i_p . Then, L_m is calculated to be higher than L_{mc} . Once the transformer parameters are calculated, then the leakage inductance L'_p of the transformer can be calculated.

For the given load resistance R_L and the transformer's turn ratio n , the quality factor Q of this LCL resonant converter can be calculated as follows

$$Q = \frac{8 \cdot n^2 \cdot R_L}{\pi^2 \cdot Z} \quad (8)$$

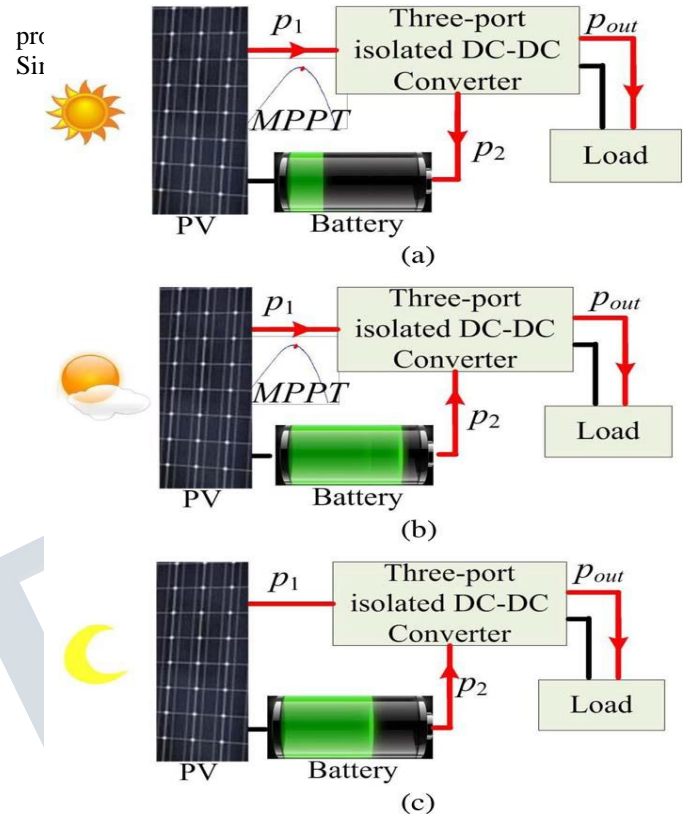
Where Z is the natural impedance of the resonant circuit defined as follows:

$$Z = \sqrt{\frac{L_r^{(k)} \parallel (L_{p1} + L'_p)}{C_r}} \quad (9)$$

Considering the necessary condition $L_p > L_r$ to achieve ZCS, $L_r = L_{p1}$ is selected, such that the currents during the switch S_1 and the transformer are close during the resonant stage.

C. Battery related Buck-Boost Converter

The buck-boost converter contains the inductor L_2 , switches S_2 and S_3 , and capacitor C_s . When the solar power generated is higher than the power required by the load, then switch S_3 is off and switch S_2 is switched on to form the buck converter. Then, the excess energy



power; the battery is charged so that the dc-link voltage is retained at a constant value. The active switches are S_1 and S_2 .

Scenario 2 ($0 < p_1 < p_{out}$): when there is low solar radiation, but the solar power is not alone sufficient to supply the load. As shown in Fig. 2(b), the PV panel is controlled in the MPPT

mode by the suggested MPPT which is described later. On the other hand, the undersupplied power is supplied by the battery, where the battery is discharged by the boost converter, so that the dc-link voltage can be maintained at a constant value. The active switches are S_1 and S_3 .

Scenario 3 ($p_1 = 0$): when there is no solar power available and thus the battery is discharged to supply the total load, as shown in Fig. 2(c). The active switches are S_1 and S_3 .

Controllers are designed properly to manage the power of the system in different scenarios.

IV. CONTROLLERS FOR DC-DC CONVERTER

A. Proposed FLC based MPPT for PV panel

In previously, P&O MPPT method is used for the of PV panel to achieve the maximum power. P&O method has the slow dynamic response and makes steady state error vary with higher sampling rates. Thus, the functioning of FLC is expected to reduce steady state error and minimizes the power losses for the converter.

Fuzzy logic controllers (FLC) works with imprecise inputs and handles nonlinearity well. The operation of FLC has four classification i.e, fuzzification, rule base, inference and defuzzification is shown in fig. 3.

Inputs to the FLC is given as error (E) and change in error (ΔE). The error (E) is calculated from (10) and change in error (ΔE) calculated from (11).

$$E = \frac{Ppv(k) - Ppv(k-1)}{Vpv(k) - Vpv(k-1)} \quad (10)$$

$$dE = E(k) - E(k-1) \quad (11)$$

Where,

$Vpv(k)$ and $Ppv(k)$ are voltage and power of the PV panel.

a) Fuzzification

Membership function values are allotted to linguistic variable using five fuzzy subsets: NB (Negative Big), NS(Negative Small), ZE(Zero error), PS(Positive small), PB (Positive big). The membership function for error, change in error and change output duty cycle are shown fig.4, fig.5 and fig.6.

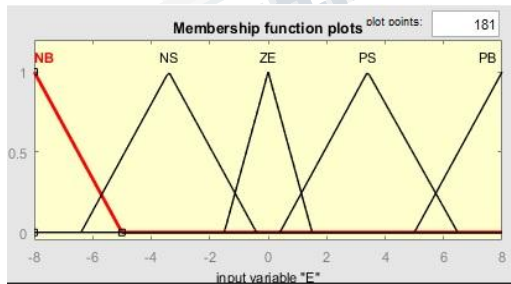


Fig.4. Membership function for error (E) input

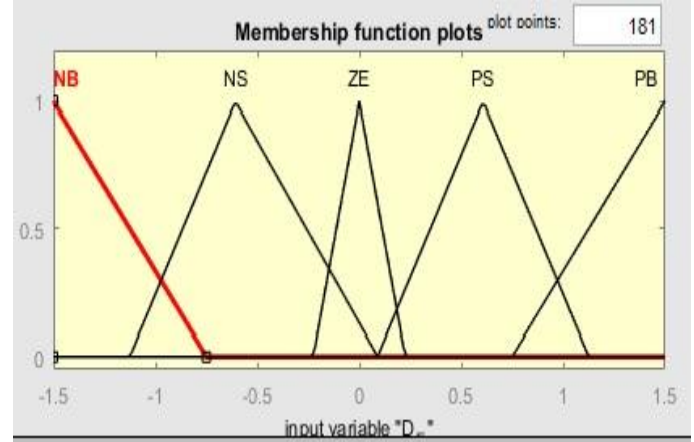


Fig.5. Membership function for change in error (ΔE) input

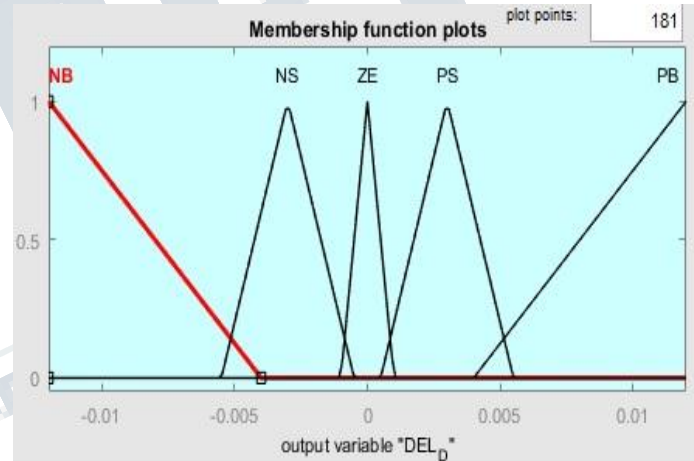


Fig.6. Membership function for change in duty cycle(ΔD)

b) Inference method

Inference is mainly consist of rule base and fuzzy implication of sub blocks. The inputs are fuzzified and given to the inference and rule base is applied. Here the mamdani type of fuzzy inference engine is used. The proposed fuzzy rule base is shown in the table I.

Table I: Fuzzy inference

Fuzzy Rule		Change in error (ΔE)				
		NB	NS	ZE	PS	PB
Error (E)	NB	ZE	PB	PB	PB	PB
	NS	PB	PS	PS	ZE	ZE
	ZE	PS	ZE	ZE	ZE	NS
	PS	ZE	ZE	NS	NS	NB
	PB	NB	NB	NB	NB	ZE

c) De-fuzzification

Centre of gravity method is used for the de-fuzzification of given inference logic to get required output of change in duty cycle. This method of defuzzification is simple and fast.

Duty ratio, the output of fuzzy logic control is given to the Pulse width modulator (PWM) generator to produce the required pulses for main switch S1.

B. Battery related Charge-discharge controller for Buck-boost converter

To control the battery current, a proportional integral (PI) control used for charge and discharge mode separately. The each separate PI controller used to produce duty cycle for the switches S2 or S3 to operate battery in charging or discharging mode. If the reference battery current is zero or negative then the charge controller get selected, the duty cycle $d2 \geq 0$ and $d3 = 0$, else the discharge controller selected, the duty cycle $d3 > 0$ and $d2 = 0$.

V. SIMULATION RESULTS

Simulations are performed in MATLAB/Simulink to validate the converter and the controllers. Specifications of the converter elements are given below:

Table II: PV panel electrical parameters

Parameter	Variable	Value
Maximum power	Pmax	54W
Voltage at MPP	Vmpp	17.4V
Current at MPP	Impp	3.15A
Open circuit voltage	Voc	22V

Short circuit current	Isc	3.3A
Total cells in series	Ns	72

Table III: Battery electrical values

Parameter	Value
Nominal voltage	7.5V
Rated capacity	5.6Ah
Internal resistance	0.16 Ω

Table IV: DC-DC converter component specification

Components	Values
L_1, L_2	320 μ H
L_m	75 μ H
L_r, L_{p1}	3.3 μ H
L'_p	0.2 μ H
C_1, C_2, C, C_s	1000 μ F
C_r	0.22 μ F
Transformer turns ratio($N_p:N_s$)	5:14
Load resistance(R_L)	100 Ω

The implementation of FLC based MPPT for three-port DC-DC converter in Simulink is shown in fig.7. The desired DC link voltage and nominal power of the converter are 50 V and 25 W, respectively.

The PV panel tested for 2.5 s with step response of different irradiance for analysis of converter and FLC controller to examine the dc link voltage and MPPT power. The PV panel power and converter dc link voltage of FLC based controller compared with P&O technique as shown in fig.9, fig.10, fig 11 and fig. 12. The same converter also tested with real time solar radiation for full day data provided by the National Renewable Energy Laboratory (NREL) [10]. The simulation duration set is 06:00 am to 18:00 pm, with resolution of one data point per hour.

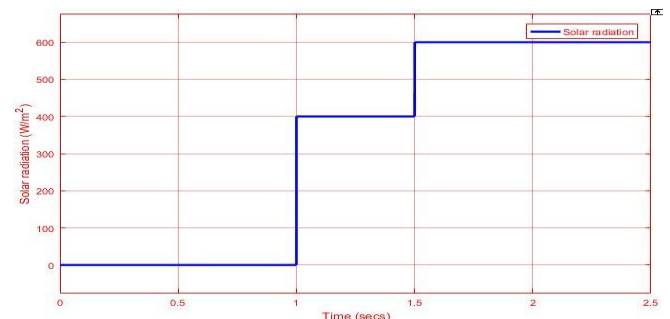


Fig. 8. Solar irradiance for the PV panel

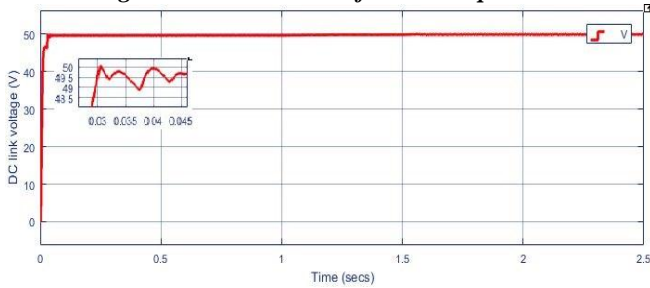


Fig. 9. DC link voltage of converter using P&O MPPT

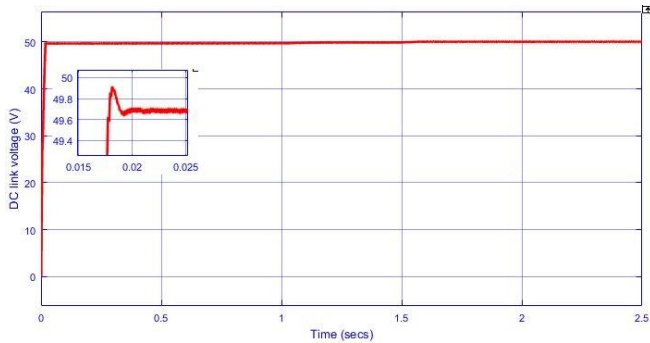


Fig. 10. DC link voltage of converter using FLC

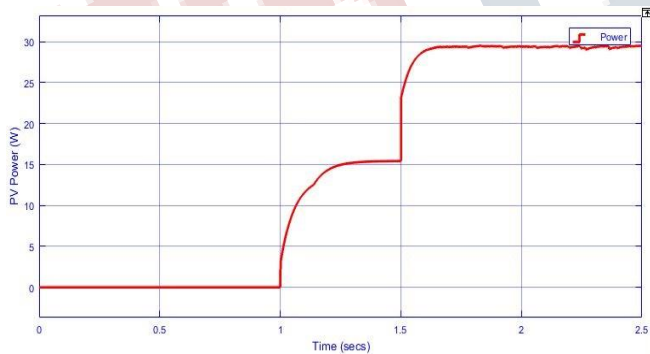


Fig. 11. PV power using P&O MPPT

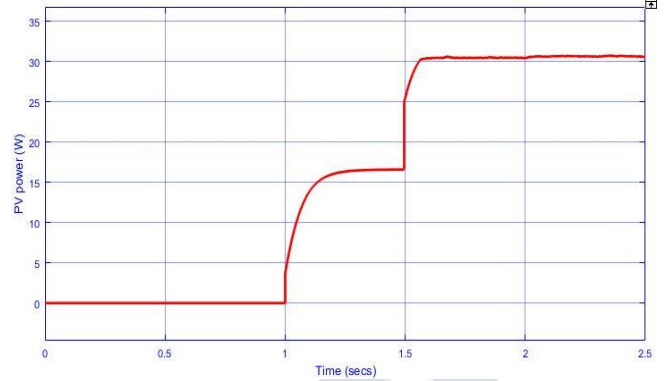


Fig. 12. PV power using FLC based MPPT

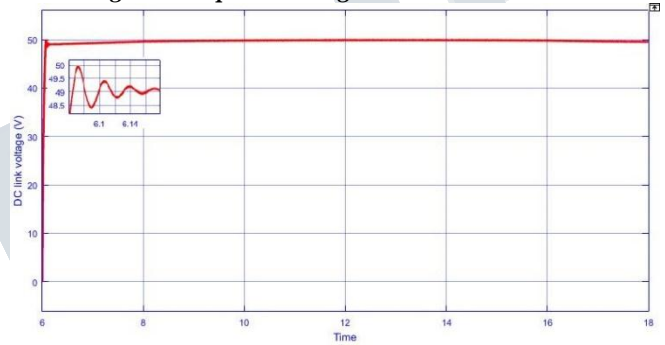


Fig. 13. DC link voltage using NREL data based on P&O

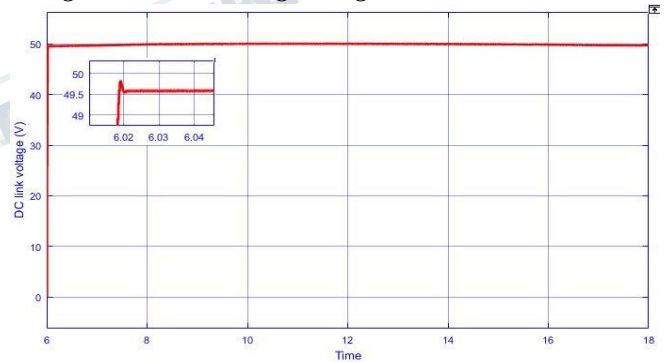


Fig. 14. DC link voltage using NREL data based on FLC

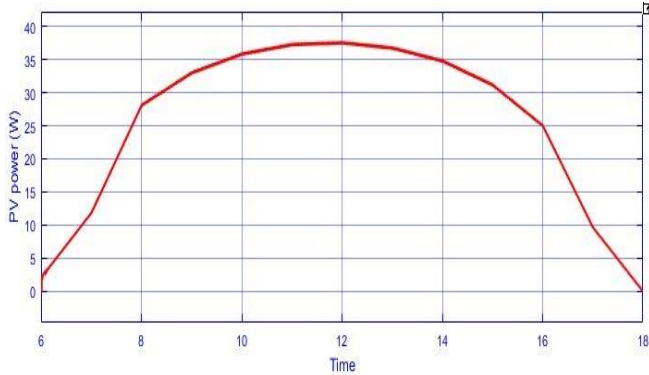


Fig. 15. Generated PV power using NREL data based on P&O

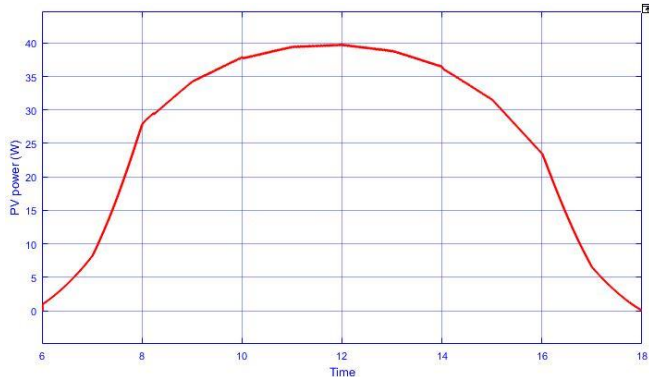


Fig. 16. Generated PV power using NREL data based on FLC

Table V: Comparison of P&O and FLC for step response data

S.No	Parameter	P&O	FLC
1	Pmax(at 600 W/m ²)	29.5 W	31W
2	DC link voltage	49.4 V	49.7 V
3	Voltage error	1.2%	0.75%

Table VI: Comparison of P&O and FLC for NREL data

S.No	Parameter	P&O	FLC
1	Pmax(at 740 W/m ²)	38 W	40 W
2	DC link voltage	49.1 V	49.65 V

3	Voltage error	1.8%	0.85%
---	---------------	------	-------

CONCLUSION

Fuzzy logic controller based MPPT is implemented for the three-port bidirectional isolated dc-dc converter with PV-battery system. Simulation results shows that FLC is capable of achieving MPPT for the PV panel and the battery is controlled in charge/discharge mode to maintain dc link voltage at a constant level. With fast convergence a small oscillations achieved by FLC method, so that the performance of FLC MPPT is better than P&O MPPT controller for the converter in terms of PV power and voltage error.

REFERENCES

- [1] C Onwuchekwa and A Kwasinski, "A modified-time-sharing switching technique for multiple-input DC-DC converters," *IEEE Trans. PowerElectron.*, vol. 27, no. 11, pp. 4492–4502, Nov. 2012.
- [2] J Lee, B Min, D Yoo, R Kim, and J Yoo, "A new topology for PV DC/DC converter with high efficiency under wide load range," in *Proc.Eur. Conf. Power Electron. Appl.*, Sep. 2007, pp. 1–6.
- [3] Y Chen, Y Liu, and F Wu, "Multi-input DC/DC converter based on the multi winding transformer for renewable energy applications," *IEEETrans. Ind. Appl.*, vol. 38, no. 4, pp. 1096–1104, Jul./Aug. 2002.
- [4] Y Lembeye, V Bang, G Lefevre, and J Ferrieux, "Novel half-bridge inductive DC-DC isolated converters for fuel cell applications," *IEEETrans. Energy Convers.*, vol. 24, no. 1, pp. 203–210, Mar. 2009.
- [5] J Zeng, W Qiao, L Qu, and Y Jiao, "An isolated multiport dc-dcconverter for simultaneous power management of multiple different renewableenergy sources," *IEEE J. Emerging Sel. Topics Power Electron.*, vol. 2, no. 1, pp. 70–78, Mar. 2014.
- [6] H Al-Atrash, F Tian, and I Batarseh, "Tri-modal half-bridge converter topology for three-port interface," *IEEE Trans. Power Electron.*, vol. 22, no. 1, pp. 341–345, Jan. 2007.

**International Journal of Engineering Research in Electrical and Electronic
Engineering (IJEREEE)**

Vol 3, Issue 9, September 2017

[7] Z Qian, O Abdel-Rahman, and I Batarseh, "An integrated four-port DC/DC converter for renewable energy application," *IEEE Trans. PowerElectron.*, vol. 25, no. 7, pp. 1877–1887, Jul. 2010.

[8] Narendrian , Sahoo, Das, and Ashwin," FLC based MPPT for PV system" , in Int. conference on electrical energy systems, 2016, pp. 29- 34.

[9] J Zeng, W Qiao, and L Qu, "A single-switch LCL-resonant isolated DCDCconverter," in *Proc. IEEE Energy Convers. Congr. Expo.*, Sep. 2013,pp. 5496–5502.

[10]. <http://www.nrel.gov/midc/apps/go2url>

